Tellus (1995), 47A, 1013–1031
Printed in Belgium – all rights reserved

TELLUS
ISSN 0280–6495

A three-dimensional baroclinic eddy-resolving model of the Baltic Sea

By ANDREAS LEHMANN, *Institut für Meereskunde, Düsternbrooker Weg 20, D-24105 Kiel, Germany*

(Manuscript received 18 May 1994; in final form 17 February 1995)

ABSTRACT

A three-dimensional eddy-resolving baroclinic model of the Baltic Sea is presented. The model comprises the whole Baltic Sea including the Gulf of Bothnia, the Gulf of Finland, Gulf of Riga as well as the Belt Sea, Kattegat and Skagerrak. With a horizontal resolution of 5 km and a discretization of 21 levels in the vertical, the general circulation and mesoscale dynamics as well as the exchange of water masses between North Sea and Baltic can be analysed. The model is forced by realistic wind fields computed from atmospheric surface pressure charts. Fresh water input due to river runoff is explicitly taken into account. At the surface, seasonal fluctuations of temperature and salinity are prescribed from a corresponding climatology. At the western boundary, an idealized North Sea basin is attached to the model domain. It is used to take up sea surface elevations in the area of the Skagerrak and to provide the water masses neccessary for the water mass exchange which have the characteristics of the North Sea. The three-dimensional initial fields of temperature and salinity were constructed from monthly mean maps of temperature and salinity and additional hydrographic measurements. Effects of vertical turbulent mixing are parameterized by using a vertical diffusion coefficient which is a function of the Richardson Number. The coefficient for horizontal diffusion of momentum is coupled with the relative vorticity. Results from different versions of the model (12/21 levels) are compared with hydrographic measurements taken during 1989 and 1992/1993. Generally, the correlation of the model solutions with the hydrographic observations is high. Most of the differences are due to uncertainties in the specified boundary conditions and forcing functions.

1. Introduction

The Baltic Sea is an almost landlocked sea in the humid climatic zone. It can be described as a large estuary with an upper layer of brackish water and a lower layer of saline water. The transition to the North Sea, the Belt Sea, with its shallow and narrow straits restricts the water mass exchange between the North Sea and the Baltic. The outflow of brackish Baltic Sea water at the surface and a compensating inflow of haline water near the bottom establish a haline stratification in the Belt Sea most time of the year (Wyrtki, 1953). Under strong west wind conditions, this stratification is broken up by mixing and a huge amount of highly saline water can penetrate into the Baltic. After passing the major sills (Drodgen and Darss sill), the highly saline water sinks down to the bottom. Its further flow through the Baltic is strongly restricted by the bottom topography. These strong inflows (Major Baltic Inflows) can change the haline stratification dramatically (Wyrtki, 1954; Matthäus and Frank, 1992). Due to high river runoff (479 km^3/year; Brogmus, 1952; Bergström and Carlsson, 1994) and a more-or-less continuous inflow of haline water originating in the Skagerrak/Kattegat, a permanent halocline in the inner Baltic is maintained. The stratification prevents an effective vertical mixing across the halocline so that a renewal of the water below the halocline is only possible by horizontal advection. During spring and summer, a seasonal thermocline develops which is eroded in autumn by turbulent mixing due to strong wind events (Krauss, 1981) and the beginning of the seasonal cooling at the surface.

Statistical analysis of infrared satellite images revealed a typical length scale of mesoscale features of about 25–60 km (Lehmann, 1992). Several observations of eddy-like structures in the Baltic showed similar scales (Aitsam and Elken, 1982; PEX-Report, 1989). The internal Rossby radius in the Baltic, which was determined to be between 2.5–10 km (Aitsam and Elken, 1982; Fennel et al., 1991), showed a strong seasonal and regional dependence. For model purposes, a high horizontal as well as vertical resolution of the model grid is required to resolve the mesoscale dynamics as well as the basin structured bottom topography and the complicated coastline with several bays and islands and the narrow and shallow straits in the transition to the North Sea.

In recent years, some numerical studies of the Baltic Sea were performed. The most recent ones are Simons (1978), Kielmann (1981), Stigebrandt (1983, 1987), Omstedt (1990), Krauss and Brügge (1991), and Gidhagen and Håkansson (1992). This list does not attempt to be complete, but it gives an impression of modeling activities in the Baltic. Most of the models presented deal with so-called box models, regional or barotropic applications, or have only low resolution. Krauss and Brügge (1991) worked with an ocean general circulation model which is similar to the model presented here.

The purpose of this study was to develop and apply a three-dimensional baroclinic eddy-resolving model of the Baltic Sea which is able to simulate most of the characteristic hydrographic features of the Baltic. The paper is organized as follows. After the Baltic Sea model equations are given, the realistic wind forcing which is calculated from atmospheric surface pressure charts and the thermohaline forcing as well as the initial conditions are presented. In Section 4, the treatment of turbulent effects is discussed. This will be followed by a comparison of model results with hydrographic observations taken during the same time range for which the wind forcing is specified. Because the intension of the paper is to demonstrate the capabilities of the Baltic Sea model, the analysis is confined to a qualitative comparison of the model solutions with hydrographic observations. A more elaborate analysis of the different experiments carried out will be published elsewhere.

2. The Baltic Sea model

The model is based on the free surface Bryan-Cox-Semtner model (Killworth et al., 1989, 1991) which is a special version of the Cox numerical ocean general circulation model (Bryan, 1969; Semtner, 1974; Cox, 1984), adapted to include a free surface. The basic equations of the model are the Navier-Stokes equations, modified in three aspects. The Boussinesq approximation is adopted in which vertical density differences are neglected except in the buoyancy term. The hydrostatic assumption is made in which local acceleration and other terms of equal order have been eliminated from the equation of vertical motion. And, lastly, closure is attained by adopting the turbulent viscosity hypotheses in which stresses exerted by scales of motion too small to be resolved by the grid are represented as an enhanced molecular mixing. The equations are written for a spherical coordinate system. Let

$$m = \sec\phi, \qquad n = \sin\phi, \qquad f = 2\Omega\sin\phi, \qquad u = a\dot{\lambda}/m, \qquad v = a\dot{\phi}, \tag{1}$$

where ϕ is latitude, λ is longitude and a is the radius of the earth. Define an advective operator Γ by:

$$\Gamma(\mu) = ma^{-1}[(u\mu)_\lambda + (v\mu m^{-1})_\phi] + (w\mu)_z. \tag{2}$$

The momentum equation then reads,

$$u_t + \Gamma(u) - fv = -ma^{-1}(p/\rho_0)_\lambda + F^u \tag{3}$$

$$v_t + \Gamma(v) + fu = -a^{-1}(p/\rho_0)_\phi + F^v, \tag{4}$$

where ρ_0 is a reference density for sea water. F^u, F^v represent turbulent effects, and are given below. The local pressure is given by the hydrostatic relation

$$p = p_s + P_a + \int_z^0 g\rho \, dz, \tag{5}$$

where p_s is the pressure at $z = 0$, and:

$$p_s = \rho_0 g\eta(\lambda, \phi, t). \tag{6}$$

η is the free surface elevation and P_a represents the surface pressure of the air. The continuity equation is

$$\Gamma(1)=0, \tag{7}$$

and the conservation of tracer T (temperature salinity and other possible tracers) is given by

$$T_t+\Gamma(T)=F^T, \tag{8}$$

where F^T represents diffusive and other effects acting on T. The equation of state is:

$$\rho=\rho(T_{is}, S), \tag{9}$$

where T_{is} is in situ temperature and S is salinity. The equation of state used here is different from the commonly used formulations (Bryan and Cox, 1972), because the density of Baltic Sea water reflects the behaviour of a typical estuary. Densities calculated from the commonly used formulations would be too low. The difference is due to fact that at a given salinity, there are more salts in the Baltic than in seawater diluted with pure water, due to the river runoff (Millero et al., 1976). Thus, the input of dissolved river salts into the Baltic has an important impact on the density. Here, it is taken into account by the relation given by Millero and Kremling (1976). Because of the small depths of the Baltic, the adiabatic effect on the temperature can be neglected. Turbulent mixing is dealt with by defining

$$\nabla^2\mu=m^2\mu_{\lambda\lambda}+m(\mu_\phi/m)_\phi. \tag{10}$$

Then the turbulent effects are

$$F^u=A_{MV}u_{zz}+A_{MH}a^{-2}[\nabla^2u+(1-m^2n^2)\,u-2nm^2v_\lambda], \tag{11}$$

$$F^v=A_{MV}v_{zz}+A_{MH}a^{-2}[\nabla^2v+(1-m^2n^2)\,v+2nm^2u_\lambda], \tag{12}$$

$$F^T=[(K_{TV}/\delta)\,T_z]_z+K_{TH}a^{-2}\nabla^2T, \tag{13}$$

where A_{MH} and A_{MV} are the horizontal and vertical mixing coefficients for momentum and K_{TH} and K_{TV} represent the corresponding coefficients for tracers. Here, vertical mixing coefficients are a function of the Richardson Number R_i. The horizontal coefficient for momentum diffusion is coupled with the relative vorticity. The rationale of this is discussed below.

Vertical mixing is handled by an infinitely rapid vertical adjustment when convective overturning could be expected. Define

$$\delta=\begin{cases}1, & \rho_z<0\\ 0, & \rho_z>0,\end{cases} \tag{14}$$

where ρ_z is the vertical gradient ignoring compressibility. The actual vertical mixing is done in a different way compared to the usually used mechanism (original Cox version). If static instability occurs, temperature and salinity of neighbouring boxes are completely exchanged only if the size of the boxes is equal, otherwise a partial mixing is done.

The lateral boundary conditions are

$$u=v=T_n=0, \tag{15}$$

where n is a normal coordinate to the wall. At the surface,

$$\rho_0A_{MV}(u_z, v_z)=(\tau^\lambda, \tau^\phi), \tag{16}$$

$$K_{TV}T_z=\mathrm{FTS}, \qquad z=0, \tag{17}$$

$$w=\eta_t+uma^{-1}\eta_\lambda+va^{-1}\eta_\phi. \tag{18}$$

τ is the wind stress and FTS represents a flux through the surface of the particular tracers involved. Effects on the tracers due to river runoff are also included in FTS. At the bottom,

$$\rho_0A_{MV}(u_z, v_z)=(\tau_B^\lambda, \tau_B^\phi), \tag{19}$$

$$T_z=0, \qquad z=-H, \tag{20}$$

$$w=-mua^{-1}H_\lambda-va^{-1}H_\phi. \tag{21}$$

The bottom friction τ_B is of second order (Cox, 1984):

$$\tau_B=\rho_0c_{db}(u^2+v^2)^{1/2}\times(u\cos\alpha-v\sin\alpha,\ u\sin\alpha+v\cos\alpha) \tag{22}$$

$$c_{db}=1.25\cdot10^{-3}, \qquad \alpha=10^0,$$

with c_{db} the drag coefficient of bottom friction and α a corresponding turning angle.

From now on, the equations are split into baroclinic and barotropic modes. Define

$$u=U/H+u', \qquad v=V/H+v', \tag{23}$$

where (U, V) is the vertically integrated (barotropic) mass flux:

$$U=\int_{-H}^{\eta} u\,\mathrm{d}z, \qquad V=\int_{-H}^{\eta} v\,\mathrm{d}z, \tag{24}$$

and (u', v') is the baroclinic flow, which possesses no depth average:

$$\int_{-H}^{\eta} u'\,\mathrm{d}z=\int_{-H}^{\eta} v'\,\mathrm{d}z=0. \tag{25}$$

The prognostic equations of the barotropic mode are defined:

$$\eta_t+a^{-1}[mU_\lambda+m(Vm^{-1})_\phi]=(P-E)/\rho_0. \tag{26}$$

In case of a mass transport through the surface, P − E represents the difference of precipitation minus evaporation. The fresh water flux A due to river runoff replaces P − E. This means, the inflow of river water into the model is considered by lifting up the free surface. The equations for the barotropic transport read,

$$U_t-fV=-ma^{-1}gH\eta_\lambda+A_{\mathrm{MH}}a^{-2}H[\nabla^2(U/H)+(1-m^2n^2)\,U/H-2nm^2(V/H)_\lambda]+X, \tag{27}$$

$$V_t+fU=-a^{-1}gH\eta_\phi+A_{\mathrm{MH}}a^{-2}H[\nabla^2(V/H)+(1-m^2n^2)\,V/H+2nm^2(U/H)_\lambda]+Y \tag{28}$$

with

$$X=-ma^{-1}(\partial/\partial\lambda)\int_{-H}^{\eta} u^2\,\mathrm{d}z-a^{-1}(\partial/\partial\phi)\int_{-H}^{\eta} uv\,\mathrm{d}z-ma^{-1}\int_{-H}^{\eta}(P_\mathrm{a})_\lambda\,\mathrm{d}z-ma^{-1}\int_{-H}^{\eta}\mathrm{d}z\int_z^0 g\rho_\lambda\,\mathrm{d}z+\int_{-H}^{\eta}A_{\mathrm{MV}}u_{zz}\,\mathrm{d}z, \tag{29}$$

$$Y=-ma^{-1}(\partial/\partial\lambda)\int_{-H}^{\eta} uv\,\mathrm{d}z-a^{-1}(\partial/\partial\phi)\int_{-H}^{\eta} v^2\,\mathrm{d}z-a^{-1}\int_{-H}^{\eta}(P_\mathrm{a})_\phi\,\mathrm{d}z-a^{-1}\int_{-H}^{\eta}\mathrm{d}z\int_z^0 g\rho_\phi\,\mathrm{d}z+\int_{-H}^{\eta}A_{\mathrm{MV}}v_{zz}\,\mathrm{d}z, \tag{30}$$

where X, Y are the definitions of the residual forcings.

The numerical model is formulated on the Arakawa B-grid. The baroclinic fields and the tracer equations are stepped forward in time with a leapfrog timestep; for the barotropic mode, an Euler backward scheme is used. A detailed description of the finite difference formulation can be found in Killworth et al. (1989).

3. Initial conditions and forcing

The model comprises the whole Baltic Sea, including Gulf of Bothnia, Gulf of Finland, Gulf of Riga as well as Belt Sea, Kattegat and Skagerrak. At the western boundary, an artificial North Sea basin is connected to the model domain to take up sea surface elevations in the area of the Skagerrak/Kattegat and to keep water masses available which have the characteristic temperature and salinity distribution of the North Sea. At the most western boundary of that basin, the sea level is adjusted to a constant reference value. In the case of a low-water level in the North Sea basin, additional water is supplied; if the water level is high, a corresponding amount is taken out of the basin. This guarantees a high water level in the area of the Skagerrak/Kattegat during strong west wind events and a corresponding low level in case of strong easterly winds. The water level in the Skagerrak/Kattegat is strongly controlled by the wind forcing on the North Sea. For a perfect simulation of the water levels in the Skagerrak/Kattegat, the whole area of the North Sea has to be taken into account with additional boundary conditions for the transitions to the North Altantic and the English Channel. Although not perfect, the simple boundary condition, specified here, circumvents the problem of the specification of unknown temperature, salinity and momentum fluxes necessary for an open boundary condition (Stevens, 1991).

The horizontal resolution of the model is 5 km (Fig. 1) and in the vertical direction 21 levels are specified (Table 1). The thickness of the different levels is chosen such as to account best for the different sill depths in the Baltic. According to the internal Rossby Radii in the Baltic, only processes of the red part of the spectrum of mesoscale motions can be resolved. A horizontal resolution in the order of the half internal Rossby Radius (at least in the order of the Rossby Radius) is required

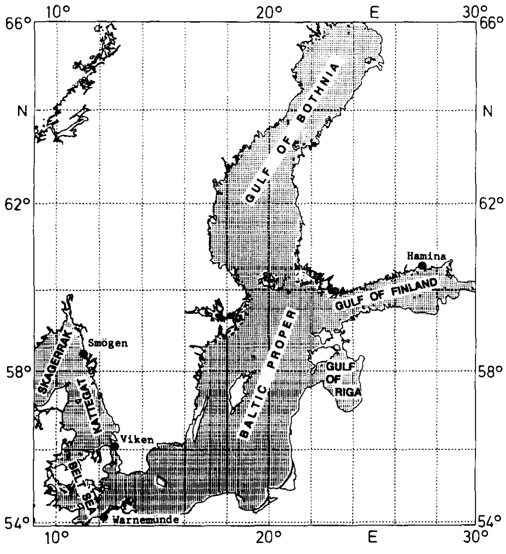

Fig. 1. Model domain and horizontal resolution (5 km).

to resolve the whole spectrum of mesoscale motions. To find a compromise between available computer resources and the resolution in space and time, the gride size of 5 km was chosen.

The three-dimensional initial fields of temperature and salinity were constructed from a monthly mean map of October (Lenz, 1971; Bock, 1971) and some additional hydrographic measurements taken during the same season. For each depth level, the data were interpolated onto the model grid by objective analysis (Hiller and Käse, 1983). The initial fields of u, v, η were set to zero. An adaption of the initial fields to model dynamics was achieved by a forward integration of the model without external forcing. After a quasi-stationary state was reached, wind forcing and climatological forcing were switched on. This technique avoids the necessity of adaptive long-term integrations to achieve a realistic distribution of temperature and salinity. To start from other initial fields, a three-dimensional distribution of

Table 1. *Baltic Sea model*

extension: 54° N–67° N 9° E–31° E	resolution: horizontal 5 km vertical 21 levels		
	Level	Depth (m)	δz (m)
forcing: realistic wind thermo-haline river runoff	1	3	6
	2	9	6
	3	15	6
	4	21	6
diffusion: turbulent viscosity hypotheses:	5	27	6
$A_{MH} = A_{MH}(\zeta)$	6	33	6
$A_{MV} = A_{MV}(R_i)$	7	39	6
$K_{TH} = K_{TH}(\zeta)$	8	45	6
$K_{TV} = K_{TV}(R_i)$	9	51	6
	10	57	6
	11	63	6
initial fields: realistic 3-d T/S	12	69	6
$u, v, \eta = 0$	13	75	6
	14	81	6
bottom friction: second order	15	87	6
	16	93	6
	17	99	6
additional tracer: oxygen	18	108.5	13
	19	127.5	25
	20	165.0	55
	21	220.0	55

temperature and salinity or other tracers taken during a synoptic hydrographic survey can be combined with one of the restart data sets of the model. For each model level, hydrographic observations of the same depth and the restart data are merged into a new initial field by using objective analysis. After an adaption of the initial fields to the model dynamics, the wind can be switched on. This procedure allows a simulation (hindcast) of the development of observed hydrographic features.

3.1. *Thermohaline forcing*

Seasonal fluctuations of temperature and salinity at the surface are prescribed from a corresponding climatology. From monthly mean surface distributions (Bock, 1971; Lenz, 1971), two-dimensional fields of temperature and salinity were constructed for each month by using objective analysis. These data were linearly interpolated in time (7.5 days interval) to achieve a smooth transition from month to month. The climatology is coupled to the model by the surface flux boundary condition (31; e.g., Bryan, 1987):

$$K_{\mathrm{TV}} T_z = \gamma\, \delta z_1 (T^* - T_1), \tag{31}$$

where δz_1 is the thickness of the uppermost model level, γ^{-1} is a damping time constant, T^* represents climatological tracer observations at the surface, and T_1 represents the tracer of the uppermost model level. A large value of γ yields a strong coupling of the first model level with the prescribed climatology, i.e., the evolution of temperature and salinity at the surface is biased to the climatology. Small values allow a free development of the surface temperature, but the seasonal change of temperature (and to a smaller extent also salinity) may be underestimated. γ can not be specified without an idea of the internal diffusion. The boundary condition keeps the climatological amount of heat and salt at the surface available; the vertical diffusion controls the absorption and internal redistribution of heat and salt. The model parameters used here can be found in Table 2. The effect of river runoff is handled by reducing the salinity in the grid box at the river mouth according to the mass transport into the model.

3.2. *Wind forcing*

At the surface, a relation for the wind stress has to be specified.

$$\tau = c_{\mathrm{d}} \varrho_{\mathrm{a}} |V_{\mathrm{w}}|\, V_{\mathrm{w}}, \tag{32}$$

with ϱ_{a} is the density of air, c_{d} the drag coefficient and V_{w} the wind speed. In the literature, one can find several formulations for the drag coefficient (Garrat, 1977; Large and Pond, 1981; Hasselmann, 1988; Blake, 1991). There is no preference for a special function for the drag coefficient. First, it was computed according to Large and Pond (33).

$$10^3 c_{\mathrm{d}} = \begin{cases} 1.14, & 4 < |V_{\mathrm{w}}| \leqslant 10 \text{ m/s} \\ (0.49 + 0.065\, |V_{\mathrm{w}}|), & 10 < |V_{\mathrm{w}}| < 25 \text{ m/s}. \end{cases} \tag{33}$$

When the simulated sea surface elevations were compared to tide gauge measurements taken at several stations around the Baltic, it turned out that the predicted amplitudes of the sea surface elevation were generally too small. The sea surface elevations showed only minor sensibility when the drag coefficient of the bottom friction (22) was varied. A better correlation of the model with observations is achieved by the modified function

Table 2. *Model parameters*

Δt_{c} (s)	Δt_{b} (s)	A_{MH} m^2/s	A_{MV} (m^2/s)	K_{TH} (m^2/s)	K_{TV} (m^2/s)	γ_{T}^{-1} day
300	7.5	$10^1 - 10^3$	$1.75 \cdot 10^{-2} - 1 \cdot 10^{-4}$	10	$5 \cdot 10^{-4} - 5 \cdot 10^{-6}$	2
γ_{S}^{-1}	b	c	β_{A}	β_{K}	n	m
20	0.5	5	15	25	2/3	1.9

(34) which amplifies the wind stress at low to moderate winds; for high wind speeds, a saturation level is reached:

$$10^3 c_d = \begin{cases} 1.54, & |V_w| \leqslant 10 \text{ m/s} \\ 1.35(1 - 0.03(|V_w| - 10)) & \\ \quad \times (0.49 + 0.065\,|V_w|), & \\ \quad 10 < |V_w| < 25 \text{ m/s}. & \end{cases} \tag{34}$$

From the Europa Modell (EM) of the German weather center in Offenbach, two-dimensional fields of air pressure at the earth's surface (every 6 h) were provided. The data have a horizontal resolution of 50 km and extend over a period from 1 January 1989 to 31 March 1990 and from 1 January 1992 to 31 December 1993. The data were interpolated in time (3-h intervals) to achieve a smooth transition from one field to the next. After that, the pressure fields were approximated by two-dimensional polynomials of 3rd order by a least square method from which a mean rms error of $\leqslant 1$ hPa (0.2 m/s) resulted. This was mainly done to save computer time and disk space. In the Baltic Sea model, the surface pressure is reconstructed from the two-dimensional polynomial and the quasi-geostrophic wind is calculated according to Bumke and Hasse (1988). The relation of surface wind (10 m) to geostrophic wind uses a constant ratio $V_{10}/V_g = 0.7$ together with an ageostrophic angle $\alpha_{ag} = 17^0$. Fig. 2 shows a quasi-geostrophic wind field and the corresponding wind stress field. The extension of the Baltic and the scale of low-pressure systems are of the same size. This means that the wind stress (Fig. 2b) varies strongly in magnitude and direction over the Baltic Sea so that at a given time, different regions of the Baltic receive a different input of energy which leads to the well-known seiches and areas of local up- and downwelling.

A comparison of wind data computed from the quasi-geostrophic approach with observations shows generally high correspondence (Fig. 3). There are only few situations where strong deviations occur. These are mainly due to features which are not present or not resolved in the surface pressure field.

A spatial average of wind velocities from 1989 is displayed in Fig. 4. The mean was computed by spatial averaging the wind vectors, taking into account only the ocean points of the model.

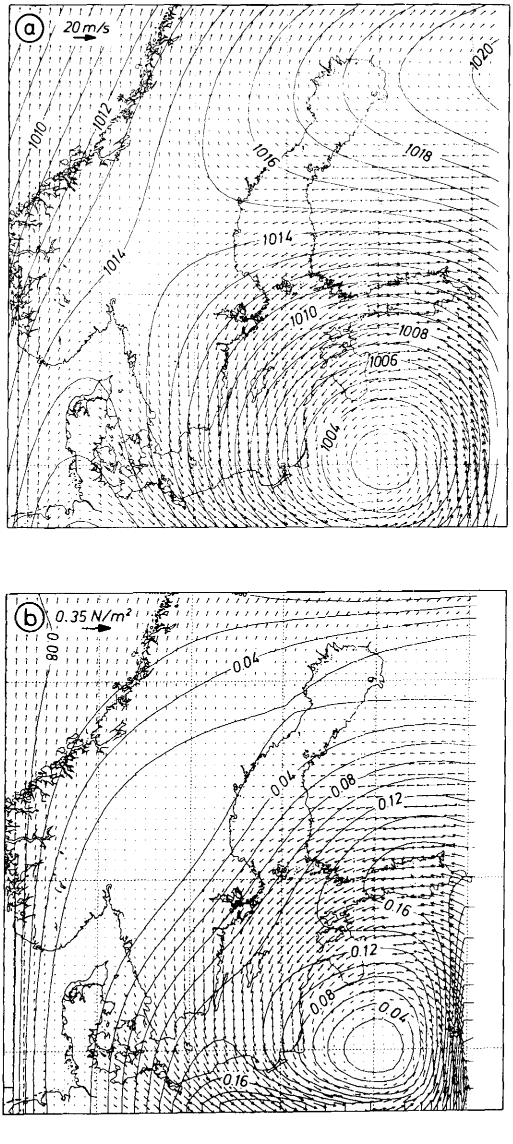

Fig. 2. (a) Surface pressure and quasi-geostrophic wind field of 31 October 1989. (b) wind stress field and absolute of wind stress, c_d calculated according to Large and Pond (1981).

Clearly, the seasonal variation in wind strength and direction can be recognized. In winter time, the winds were as strong as 19 m/s from almost western directions. From March until August, the wind velocities only occasionally reached 10 m/s. During that time, the wind direction showed the

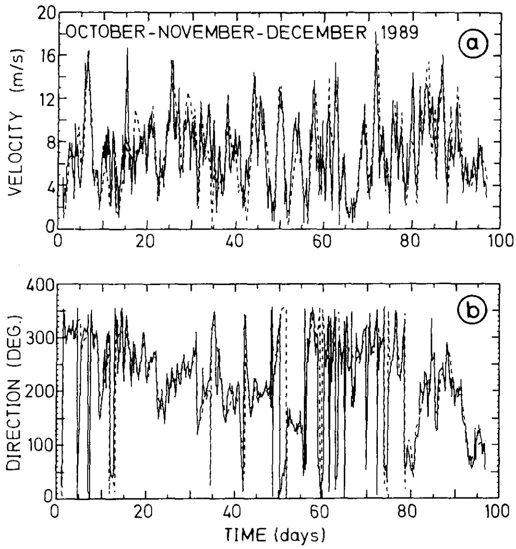

Fig. 3. Observed wind velocities (full line) and computed wind velocities (dashed line) at 59°19.9′N, 10°58.1′E.

highest variability. Towards the end of the year, the wind speed increased again (14 m/s) with prevailing wind directions from the west. Considerable deviations from these averaged values could occur. In January, in the area of the Skagerrak, wind speeds were as high as 25 m/s. This means that during autumn and winter, an inflow of haline water originating from the Skagerrak/Kattegat can be expected. During spring and summer, outflow situations occur predominatly. Over most times of the year, the Belt Sea area shows a haline stratification, but during heavy storms, the whole water column can be mixed completely by turbulence, and an inflow of a huge amount of highly saline water can occur (Wyrtki, 1954). During summer and late summer, heavy storms can lead to an erosion of the thermocline (Krauss, 1981).

3.3. *Air pressure gradient*

The air pressure gradient at the surface has to be taken into account as an additional forcing acting on the Baltic Sea. Kielmann (1981) showed that due to the spatial distribution of the surface pressure, seiches of low order were excited in the Baltic which had maximum amplitudes of 0.2 m. The horizontal gradient of the surface pressure affects the whole water column and forces a barotropic current. The relative strength of the pressure gradient depends on water depth. If the gradient is multiplied by the mean water depth of the Baltic (55 m), a corresponding stress field can be computed (Fig. 5). If the air pressure gradient is considered as an additional forcing, the combined

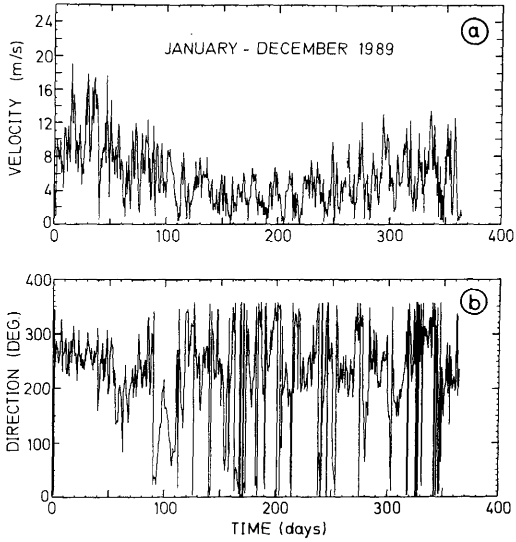

Fig. 4. Time-series of the spatial average of wind velocities over the Baltic Sea.

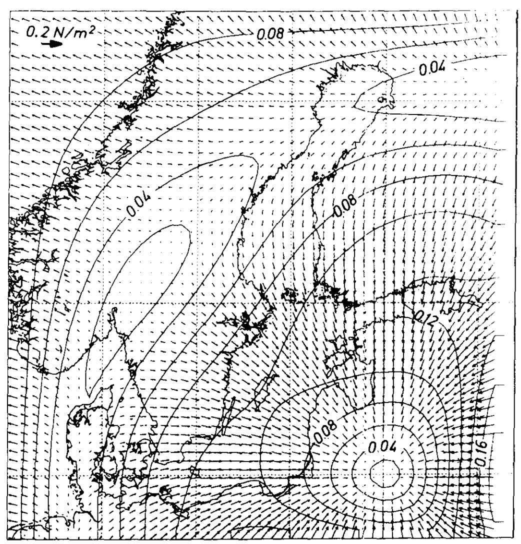

Fig. 5. Apparent stress field due to air surface pressure effects.

stress vector (wind stress (Fig. 2b) and air pressure gradient) is turned to the left in the direction of the low pressure.

4. Diffusion and friction

Mixing processes deeply affect the baroclinic structures in the ocean. How far these processes are resolved by the model dynamics depends primarily on the horizontal and vertical resolution of the model grid. If the horizontal resolution is suitable to resolve the mesoscale dynamics explicitly, the diffusion coefficients parameterize only subscale processes. Furthermore, the horizontal eddy viscosity is determined from computational considerations. It cannot be arbitrarily small for a given grid size, because computational noise arises if A_{MH} is below a critical value. The numerical dispersion of the advection scheme can lead to an unphysical behaviour of the advected quantities (Gerdes et al., 1991). Due to the realistic wind forcing which ranges from low to very high wind speeds, up to 25 m/s, in local areas, especially near the coast, dispersive effects could be observed. To suppress these effects, a suitable diffusion has to be prescribed. It would be desirable if the horizontal diffusion coefficient were coupled with the turbulent state of the sea. A coupling of the horizontal mixing with the relative vorticity ζ seems to be appropriate. The relation for the coefficient of the horizontal diffusion of momentum can be defined:

$$A_{\mathrm{MH}} = \begin{cases} 10\ \mathrm{m^2/s}, & |\zeta| < 1 \cdot 10^{-8} \\ 10^{c}\,|\zeta|^{b}, & 1 \cdot 10^{-8} \leqslant |\zeta| \leqslant 1 \cdot 10^{-4} \\ 1 \cdot 10^{3}\ \mathrm{m^2/s}, & |\zeta| > 1 \cdot 10^{-4} \end{cases} \tag{35}$$

with $\zeta = v_x - u_y$ and b, c are constants (Table 2) determined from statistical considerations. In a pre-experiment, histograms of relative vorticity were calculated. To the range between minimum and maximum, a function for the diffusion coefficient was fitted. In regions where high relative vorticity occurs, the diffusion coefficient reaches a maximum value so that dispersive effects are successfully damped out. An alternative to this kind of diffusion may be the application of an high selective biharmonic operator (Holland, 1978). The corresponding coefficient for biharmonic diffusion can be chosen to give the same control of computational noise, while drastically cutting down the diffusion of features having mesoscale wavelength (Semtner and Mintz, 1977). A comparison of biharmonic diffusion with the above proposed form will be carried out in future model calculations. However, some tests have been made which showed that model runs, for which the diffusion was coupled with the relative vorticity, were more robust when starting the model from objective analysed data.

Vertical mixing in the upper oceanic layer provides the mean exchange of heat, water and momentum between the atmosphere and the deeper ocean. Vertical momentum diffusion controls major dynamical features of the ocean interior. Due to the shallow water approximation, the vertical momentum balance reduces to the hydrostatic relation. Hence, vertical turbulence cannot be simulated at all. A more-or-less sophisticated vertical diffusion scheme has to be introduced to parameterize vertical mixing at all depths from the upper boundary to the bottom. A summary of recent vertical mixing schemes is given by Gaspard et al. (1990). Following Munk and Anderson (1948) and Pacanowsky and Philander (1981), a Richardson number dependent vertical diffusion scheme is used here. The diffusion coefficients are defined by:

$$A_{\mathrm{MV}} = \mathrm{MAX}\left(\frac{A_0}{(1+\beta_{\mathrm{A}} R_{\mathrm{i}})^{n}},\, A_{\min}\right) \tag{36}$$

$$K_{\mathrm{TV}} = \mathrm{MAX}\left(\frac{K_0}{(1+\beta_{\mathrm{K}} R_{\mathrm{i}})^{m}},\, K_{\min}\right) \tag{37}$$

with

$$R_{\mathrm{i}} = \frac{N^2}{|\partial u/\partial z|^2}, \qquad N^2 = \frac{g}{\rho_0}\frac{\partial \rho}{\partial z}.$$

For numerical stability, the diffusion must be bounded. $A_{\min}$, $K_{\min}$ specify the minimum, and A_0, K_0 the maximum values of the range the diffusion can take. β_{A}, β_{K}, n and m are parameters to adjust the vertical diffusion (Table 2).

Krauss (1981) showed that during heavy storms in the Gotland Basin, strong inertial waves and vertical current shears were excited which reduced the Richardson number within the thermocline to values around 0.25. A Richardson number of this size is a strong indicator that internal waves, which are always present in the thermocline, must break leading to vigorous vertical turbulent mixing. The parameters of (36, 37) were chosen to simulate this effect. The water column will be vertically mixed if $R_i < 0.25$, i.e., the vertical diffusion must reach maximum values. Due to computational reasons, a suitable diffusion must be prescribed if $R_i \gg 0.25$. The stratification in the model is very sensitive to different parameters of the function of the vertical diffusion.

Matthäus (1977) calculated for the Baltic Proper, from mean annual variations of temperature, averaged coefficients of the vertical turbulent heat exchange for 10-m layers. The results were related to the vertical stability. In a stably stratified water column, a diffusion of $< 10^{-5}$ m^2/s can be expected. Moderate stability leads to values of $10^{-4} - 10^{-3}$ m^2/s. Under unstable or turbulent conditions, the diffusion ranges between $10^{-3} - 10^{-2}$ m^2/s. The values prescribed in the model cover the range for a stably stratified water column to moderate stability (Table 2). Unstable conditions are handled by the vertical convection scheme.

5. Model results and model verification

The model can be used to simulate general circulation, mesoscale dynamics, mixed layer dynamics, water mass exchange between North Sea and Baltic as well as the exchange between the deep basins, Major Baltic inflows, drift studies, etc. To demonstrate the capabilities of the model, results from different simulations are presented. A verification of the solutions obtained is possible if hydrographic observations are available for the time range for which the realistic wind forcing is specified. Because wind data for 1989 and 1992/1993 are already prepared to force the model, the simulations focus on these particular years. The model run for 1989 is based on an earlier version of the Baltic Sea model with 12 levels in the vertical, no river runoff and a different western boundary condition. In this version, there is also an artificial North Sea basin connected to the model domain, but no adjustment of the sea surface elevation is made (Lehmann, 1992). The introduction of the quasi-open boundary condition in the more recent model version improved the simulation of surface elevations in the area of the Skagerrak/Kattegat. Furthermore, the inflow (Major Baltic Inflow) of highly saline water after periods of persistent and strong westerly winds which cause large sea-level differences between the Skagerrak and the western Baltic is governed by the barotropic pressure gradient. This means that a considerable improvement of the simulation of the water mass exchange between North Sea and Baltic can be expected. The increase of the vertical resolution was mainly done to utilize the vertical convection scheme. For equal vertical grid size, neighbouring water masses can simply be exchanged without mixing if static instability occurs. Furthermore, the numerical vertical diffusivity K_{num} in a numerical model with non-uniform grid can lead to an unphysical negative value (Yin and Fun, 1991). In a downwelling region, the numerical diffusivity is negative for a grid with grid size increasing with depth. When the grid size increment, or the downward vertical velocity is large, K_{num} may exceed the vertical diffusivity specified and may result in an effective negative vertical diffusivity.

5.1. General circulation

Because of the high annual variability of the meteorological and hydrographic parameters over the Baltic (e.g., development of the thermocline, ice cover, wind forcing), it may be difficult to extract a representative mean circulation of the whole Baltic Sea. Fig. 6 shows the mean barotropic (vertically integrated) transport for May and October, 1989. In May, generally, calm weather conditions prevail, whereas in October, strong winds mainly from western directions can be expected. In springtime, the barotropic transport is determined by the thermohaline circulation; in autumn, the mean circulation is strongly influenced by strong westerly winds. As a consequence, the mean barotropic transports for the different seasons show different circulation patterns. The vertically integrated transports are comparable with the transports calculated in Kielmann (1981). Due to the varying wind conditions and to a lower extent to the river runoff, the mean water content of the Baltic oscillates. The water content can be expressed by the mean sea level of the Baltic

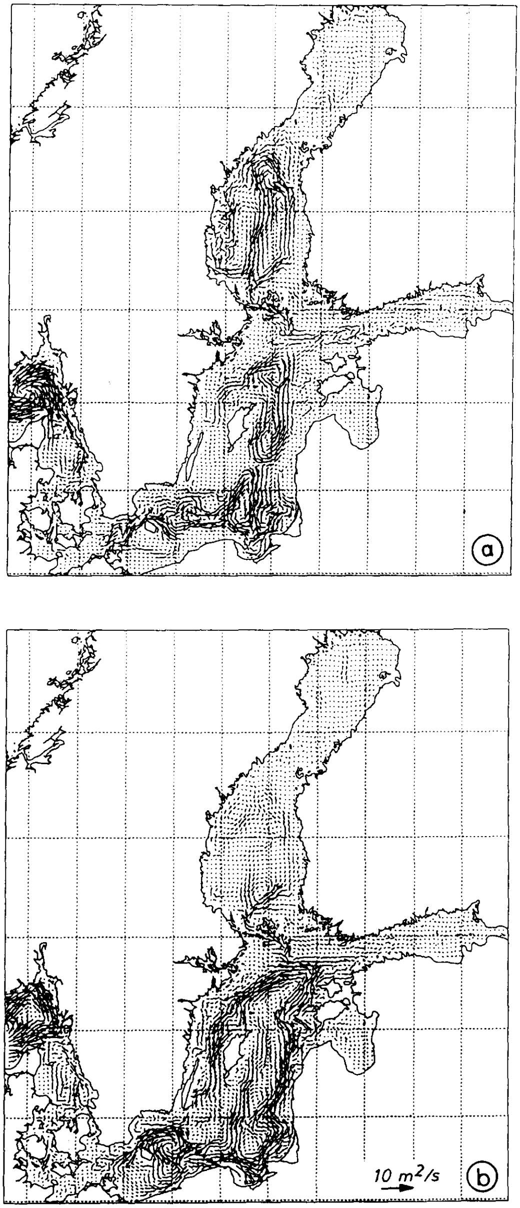

Fig. 6. Mean barotropic circulation (a) May 1989 and (b) October 1989.

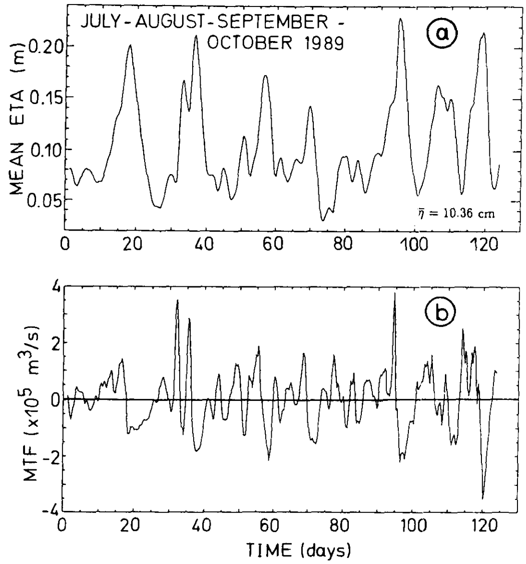

Fig. 7. Time-series (a) of the mean sea level of the Baltic Sea and (b) the corresponding barotropic mass transport through the Danish Straits.

(Fig. 7). Between the extrema, effective inflow or outflow situations occur which can last more than 5 days. The corresponding mass transports (Fig. 7b) are quite comparable with observed transports through the Belt Sea (Jacobsen, 1986).

5.2. *Sea surface elevation*

A comparison of tide gauge measurements with simulated sea surface elevations allows a verification of the barotropic response of the model. The amplitudes and phases of the surface elevations are mainly influenced by the wind stress and the bottom friction. Fig. 8 shows sea surface elevations for two stations in the Baltic and the Kattegat/Skagerrak from October until December 1989. In the Baltic, the correspondence of simulated surface elevations and observations is very high, whereas, in the Kattegat/Skagerrak, larger differences can be observed. Obviously, these discrepancies are due to a wrong behaviour of the western boundary condition (12-level version). The water mass exchange between North Sea and Baltic through the Belt Sea is governed by the sea level difference between the Kattegat and western Baltic and frictional forces. For positive sea level differences, inflow occurs; negative differences result in an outflow. Fig. 9 shows a comparison of simulated and observed sea level differences between Kattegat and western Baltic from July until December 1989. Most of the inflow/outflow events are correctly predicted, but the amplitudes of the simulated sea level differences are generally too small.

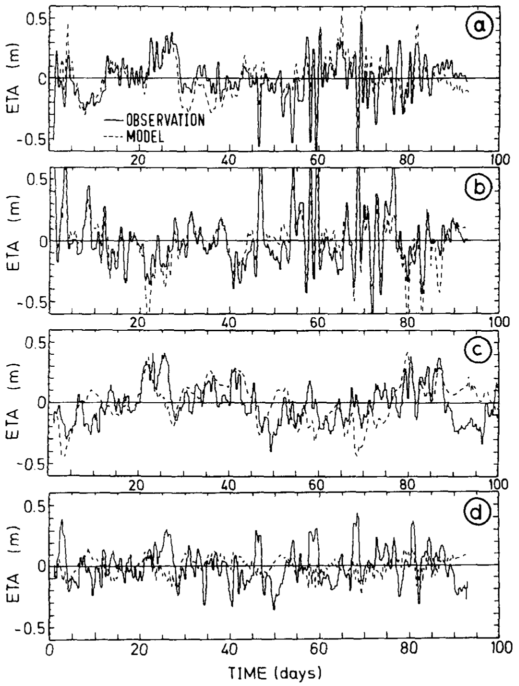

Fig. 8. Time-series of sea surface elevation for (a) Hamina, (b) Warnemünde, (c) Smögen and (d) Viken, observations: full line, model: dashed line.

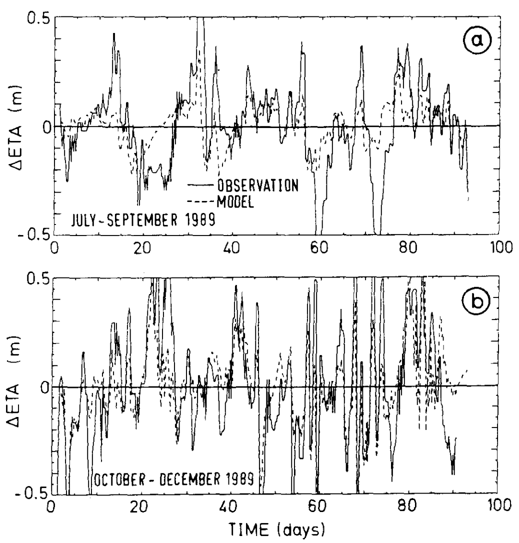

Fig. 9. Sea level difference between Kattegat and western Baltic, observations (full line), model (dashed line).

From statistical considerations, it was determined that a sea level difference of 0.1 m results in a barotropic transport of $5 \cdot 10^3\,m^3/s$ (Lehmann, 1992). It should be noted that an underestimation of the barotropic transport through the Belt Sea results in an underestimation of the salt budget of the Baltic Sea, i.e., the haline stratification can be too weak.

5.3. *Stratification*

The vertical distribution of salinity is primarily determined by horizontal advection and diffusive processes, whereas the thermal stratification is mainly controlled by the heat flux through the surface which shows a high annual variability. In spring, a shallow thermocline develops which deepens during summer. In autumn, this thermocline is eroded by turbulent mixing and vertical convection due to cooling at the the surface. During winter, vertical convection intensifies until it covers the whole water column down to the permanent halocline.

The development of the stratification described above is fairly well reproduced by the model. The evolution of the seasonal thermocline can be observed in a section through Kattegat, Belt Sea and Baltic Sea (Fig. 10). In the Baltic, a halocline separates a less haline water body ($\leqslant 8$ psu) from horizontally advected saltier water masses (10–12 psu). This halocline persists during the year. It should be noted that due to a wrong behaviour of the western boundary condition (12-level version), the vertical salinity distribution is biased to too low salinities in the deeper parts of the Bornholm and Gotland Sea (Fig. 10d–f). Normally, the mean salinity in the Bornholm Deep ranges between 15–17 psu.

5.4. *Currents*

It is always a problem to compare simulated baroclinic currents with observations. A moored current meter provides a point measurement, whereas the currents calculated by the model represent an integral estimation dependent on the model resolution. In the narrow and shallow Danish Straits, mainly two current directions prevail, which corresponds to inflow and outflow situations. Furthermore, the narrowness of the Belt Sea amplifies these currents (0.5–1 m/s; Wyrtki, 1953) so that small-scale fluctuations are mainly suppressed. A disadvantage may be the

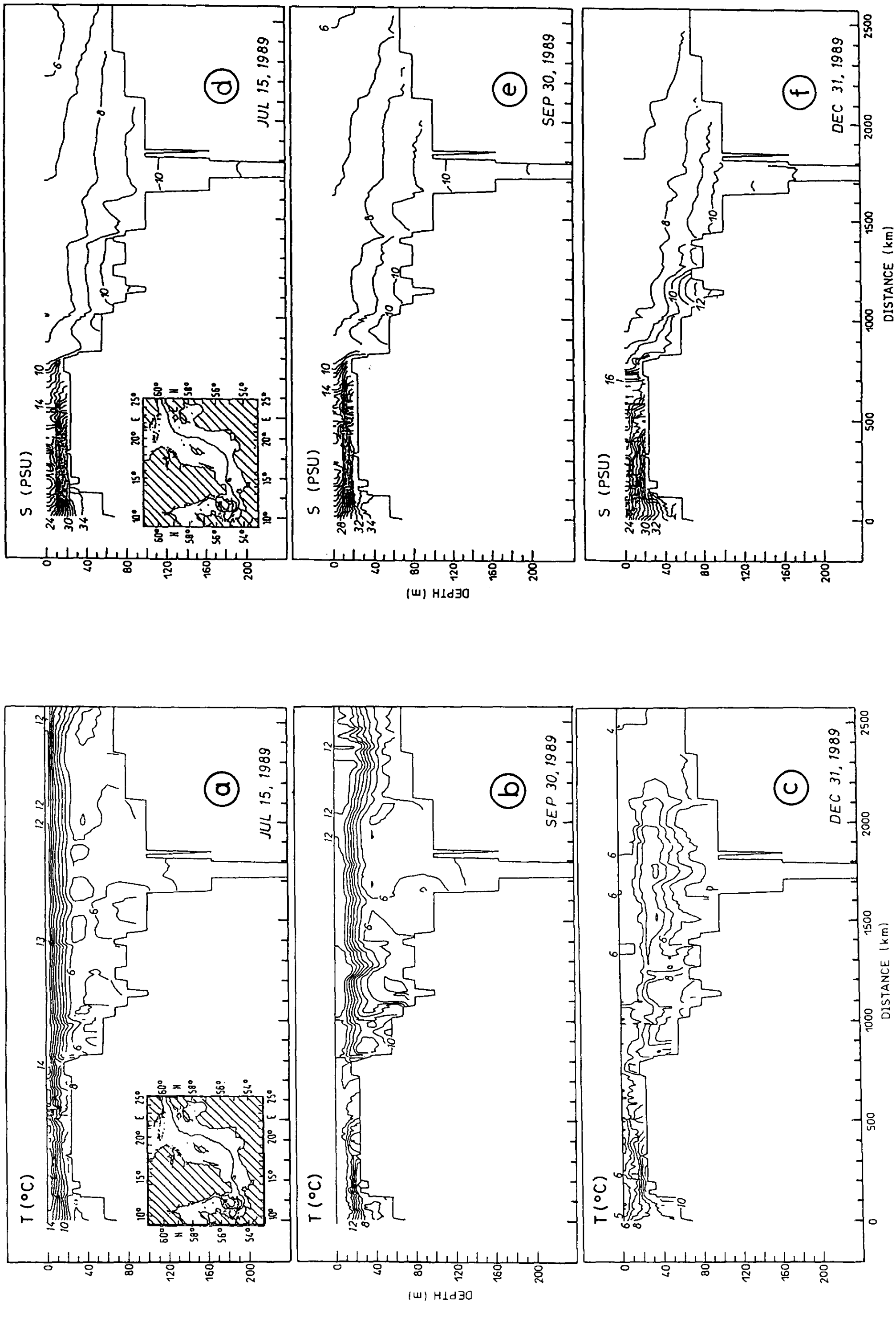

Fig. 10. Evolution of the vertical distribution of temperature (a–c) and salinity (d–f) in a section through the Baltic Sea.

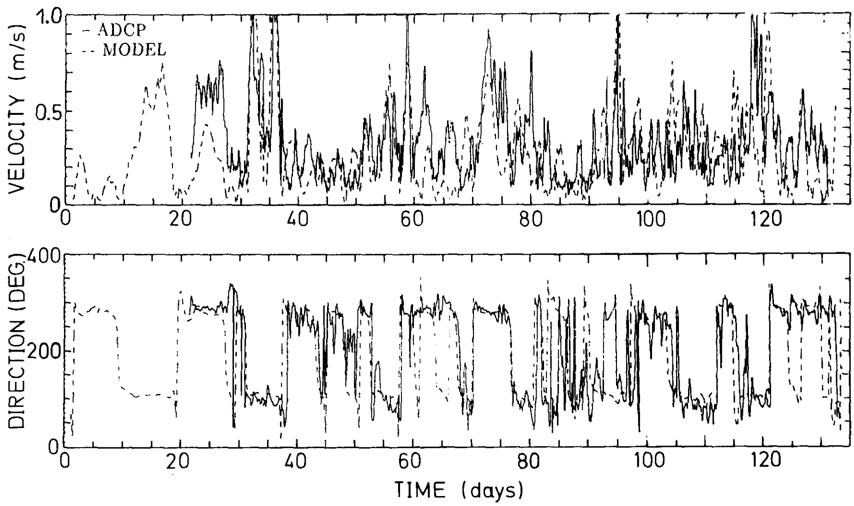

Fig. 11. Time-series of current velocity at Fehmarn Belt from July to October, 1989: ADCP (full line), model (broken line).

tides in the area of the Belt Sea. The sea surface elevations due to diurnal and semi-diurnal tides are of the order of 0.1 m, with corresponding currents of 0.3–0.4 m/s (Wyrtki, 1953; Magaard and Rheinheimer, 1974).

Two periods (27 January 1989 to 4 April 1989 and 21 July 1989 to 7 November 1989) of ADCP measurements in the Fehmarn Belt exist for 1989. A comparison of measurements of the second period with simulated currents is displayed in Fig. 11. Most of the inflow and outflow situations are correctly covered by the model. The amplitudes of the currents are generally of the same order. The differences between simulation and observation may be due to errors in the specified wind forcing and a wrong behaviour of the western boundary condition. Nevertheless, the correspondence is high which is also confirmed by statistical considerations (Fig. 12). Because the currents in the Fehmarn Belt are mainly zonally directed, the power density of the u-component is considerably higher than the v-component. For periods shorter than 2 days, the higher energy level of the observations is probably due to tidal effects.

5.5. *Major Baltic inflow in January 1993*

During recent decades, several major inflows of highly saline water into the Baltic occurred. These events took place mostly in autumn or in early winter time and lasted between a few days up to 29 days (Matthäus and Franck, 1992). The most recent inflow occured in 1993. After 16 years of stagnation, this major inflow which was found to be a moderate one, transported 125 km^3 of highly saline and oxygenated water into the Baltic Sea.

A detailed hydrographic description of the inflow in January 1993 and the impact on the Baltic can be found by Dahlin et al. (1993), Håkansson et al. (1993) and Matthäus et al. (1993).

The major inflow in January 1993 was simulated with the 21-level version of the Baltic Sea model. The experiment was started from a three-dimensional mean distribution (October) of temperature and salinity. The wind forcing was specified for the range from 1 October 1992 to 31 March 1993. Fig. 13 displays a transect of salinity through the Belt Sea, Arkona Sea and Bornholm Sea to compare the simulated vertical salinity distribution with observations taken during a hydrographic survey of R. V. Alkor in March 1993. Generally, the salinity distributions look very similar, except in the Arkona Basin, where higher deviations appear. The depth of the mixed layer is underestimated by the model. As a consequence, the vertical gradient of salinity across the halocline is too weak. The corresponding TS-diagram (Fig. 14) reveals an acceptable salinity distribution, but the temperature in the upper layers is somewhat too high, which can be due to uncertainties in the specified diffusivities and heat flux at the surface.

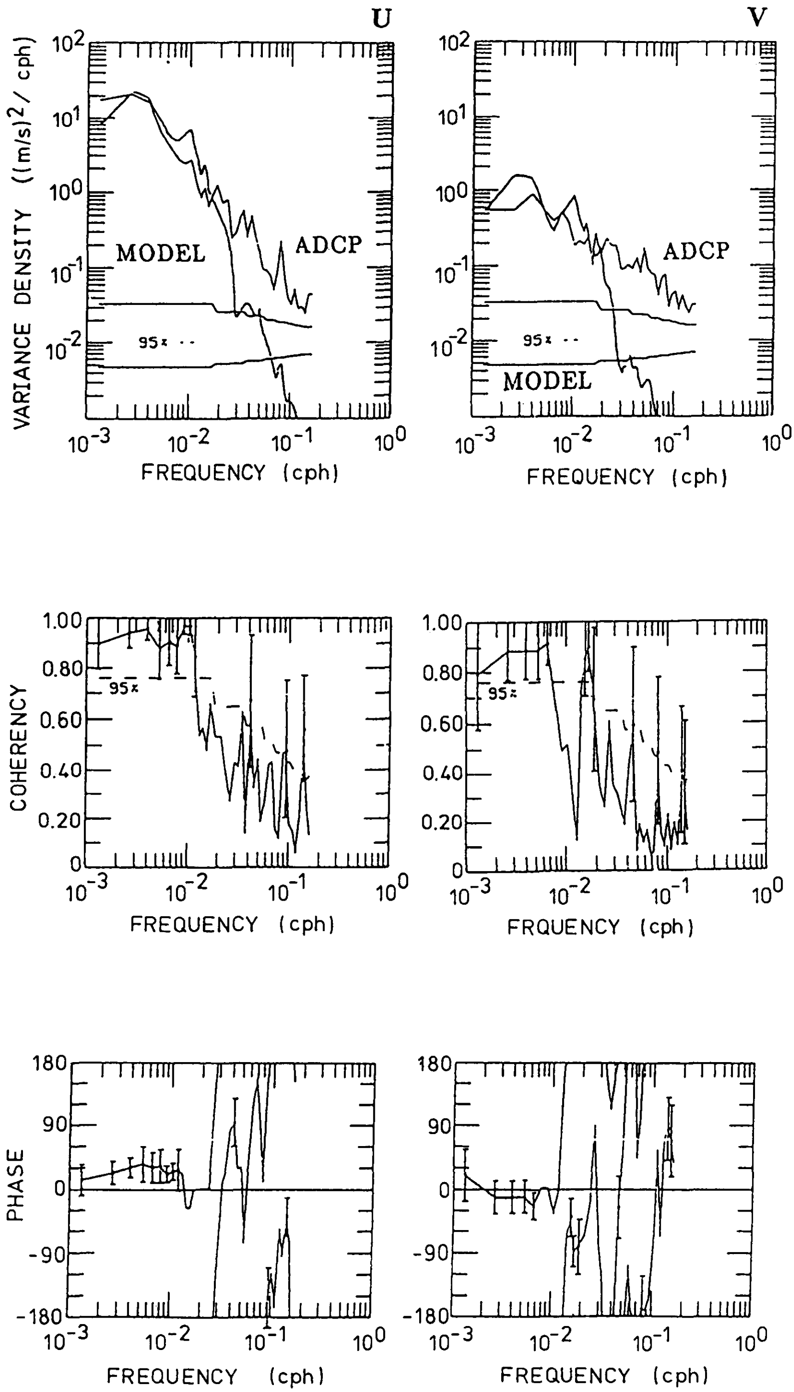

Fig. 12. Power density spectrum, coherency and phase of measured (ADCP) and simulated current velocity at the Fehmarn Belt.

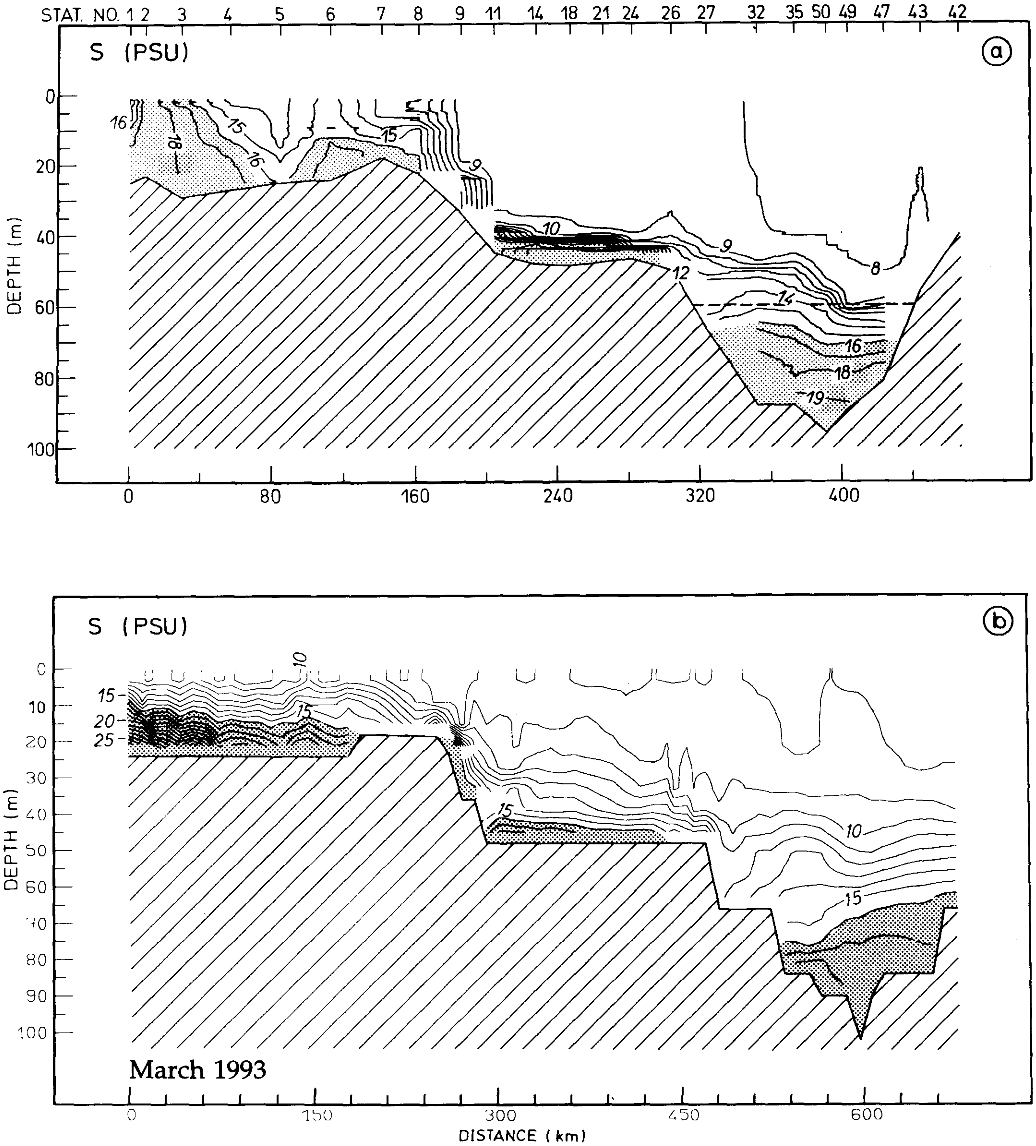

Fig. 13. Section of salinity through the Belt Sea, Arkona Sea and Bornholm Sea, March, 1993, (a) observation, (b) model.

6. Summary and conclusions

A three-dimensional eddy-resolving baroclinic model of the Baltic Sea is presented. The horizontal resolution is 5 km and the topography of the Baltic is approximated by (12) 21 levels. The initial conditions are realistic three-dimensional distributions of temperature and salinity. With realistic forcing functions, a verification of the model with hydrographic observations is possible. The focal point of this study is the development of a model which is able to simulate most of the baroclinic

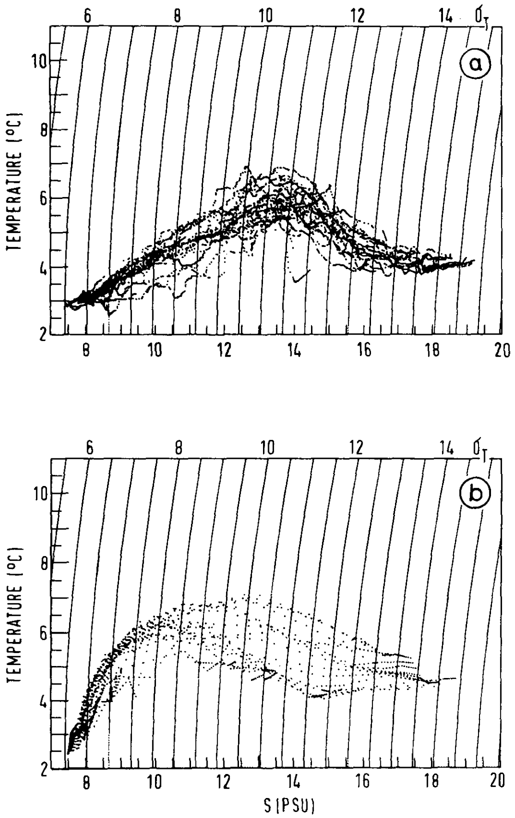

Fig. 14. TS-diagram of the Bornholm Sea, March 1993, (a) observations, (b) model.

structures of the Baltic Sea with particular emphasis on the response of the thermohaline circulation. The verification of the model solutions with different hydrographic parameters provides generally high correspondence. A comparison of tide gauge measurements with simulated sea surface elevations reveals high correlations in the Baltic, but due to the western boundary condition, the simulation in the Kattegat/Skagerrak is rather weak (12-level version). From an integration over a whole year, which was performed to take the seasonal developement of the thermocline into account, the resulting stratification shows most features of the Baltic Sea. During summer, a thermocline develops which is eroded in autumn by turbulent mixing and vertical convection due to cooling at the surface. In winter time, the formation of the cold winter water can be observed. The permanent halocline of the Baltic is maintained by the river runoff and horizontal advection of saline water from the Kattegat. The magnitude of inflow of highly saline water originating in the Kattegat/Skagerrak is strongly controlled by the wind conditions over the North Sea and Baltic Sea. A simulation of the Major Baltic inflow in January 1993 results in a realistic distribution of salinity.

The main problem of the model calculations is to find suitable parameterizations of the inherent turbulent processes, which are not explicitly resolved by the model dynamics. The coupling of the horizontal eddy viscosity with the relative vorticity provides encouraging results. On the one hand, dispersive effects are successfully depressed and on the other hand, in regions of low relative vorticity, the eddy viscosity is small, so that abundant damping of mesoscale dynamics is avoided. The solutions of the model show a great sensitivity to the magnitude (functional dependence) of the vertical diffusivity, which strongly controls the stratification of temperature and salinity and hence the occurrence of a major inflow to the Baltic. This means that the salt budget of the Baltic Sea is also controlled by the vertical diffusion. Furthermore, the magnitude of the surface heat and salt fluxes increases with increasing diffusivity. Another problem arises from uncertainties in specifying the correct fluxes at the surface, because the physics of the processes involved are not fully understood. Some problems for the water mass exchange through the Belt Sea may arise from the horizontal resolution of the model. An increase in the horizontal resolution or the application of a nested grid would probably lead to more realistic mass transports.

Nevertheless, the model is suitable for simulation of general circulation, mesoscale dynamics, mixed-layer dynamics, water-mass exchange between the North Sea and the Baltic as well as the exchange between the deep basins. For the future, an improvement of the mixed-layer dynamics, a combined ice-ocean model as well as a coupling of atmosphere and ocean is planned.

7. Acknowledgements

This work is a contribution to the Baltic Sea Experiment (BALTEX) and was supported by the Deutsche Forschungsgemeinschaft (DFG).

REFERENCES

Aitsam, A. and Elken, J. 1982. *Synoptic scale variability of hydrophysical fields in the Baltic proper on the basis of CTD measurements. Hydrodynamics of semi-enclosed seas.* J. C. C. Nihoul, Editor, Elsevier, Amsterdam, 433–468.

Bergström, S. and Carlsson, B. 1994. River runoff to the Baltic Sea: 1950–1990. *Ambio* **23** (nos. 4–5), 280–287.

Blake, R. A. 1991. The dependence of wind stress on wave heigth and wind speed. *J. Geo. Res.* **96** (no. C11), 20531–20545.

Bock, K. H. 1971. Monatskarten des Salzgehaltes der Ostsee. *Ergänzungsheft zur Hydrographischen Zeitschrift*, Reihe ***B***, no. 12.

Brogmus, W. 1952. Eine Revision des Wasserhaushaltes der Ostsee. *Kieler Meeresforsch.* **9**, 15–42.

Bryan, F. 1987. Parameter sensitivity of primitive equation ocean general circulation models. *J. Phys. Oceanogr.* **17**, 970–985.

Bryan, K. 1969. A numerical method for the study of the circulation of the world ocean. *J. Phys. Oceanogr.* **15**, 1312–1324.

Bryan, K. and Cox, M. D. 1972. An approximate equation of state for numerical models of ocean circulation. *J. Phys. Oceanogr.* **2**, 510–514.

Bumke, K. and Hasse, L. 1989. An analysis scheme for the determination of true surface winds at sea from ship synoptic wind and pressure observations. *Boundary-Layer Met.* **47**, 295–308.

Cooperative Research Report, 1989. *Baltic Sea Patchiness Experiment PEX-86*. International Council f. the Exploration of the Sea, Denmark.

Cox, M. D. 1984. *A primitive equation 3-dimensional model of the ocean*. GFDL Ocean Group Tech. Rep. No. 1, GFDL/Princeton University.

Dahlin, H., Fonselius, S. and Sjöberg, B. 1993. *The changes of the hydrographic conditions in the Baltic proper due to 1993 major inflow to the Baltic Sea.* ICES 1993 C.M. 1993/C:58.

Fennel, W. 1991. Rossby radii and phase speeds in the Baltic Sea. *Cont. Shelf Res.* **11** (no. 1), 23–36.

Garrat, J. R. 1977. Review of drag coefficients over oceans and continents. *Mon. Wea. Rev.* **105**, 915–929.

Gaspar, P., Gregoris, Y. and Lefevre, J. 1990. A simple eddy kinetic energy model for simulations of the oceanic vertical mixing: tests at station Papa and long-term upper ocean study site. *J. Geo. Res.* **95** (C9), 16179–16193.

Gerdes, R., Köberele, C. and Willebrand, J. 1991. The role of numerical advection schemes on the results of ocean general circulation models. *Clim. Dyn.* **5**, 211–226.

Gidhagen, L. and Håkansson, B. 1992. A model of the deep water flow into the Baltic Sea. *Tellus* **44A**, 414–424.

Håkansson, B., Broman, B. and Dahlin, H. 1993. *The flow of water and salt in the Sound during the Baltic major inflow event in January 1993.* ICES C.M. 1993/C:57.

Hasselmann, S. et al. (WAMDI GROUP) 1988. The WAM Model-A third generation ocean wave prediction model. *J. Phys. Oceanogr.* **18**, 1775–1810.

Hiller, W. and Käse, R. H. 1983. Objective analysis of hydrographic data sets from mesoscale surveys. *Ber. Inst. f. Meeresk.* (Kiel) (no. **116**), 78 pp.

Holland, W. R. 1978. The role of mesoscale eddies in the general circulation of the ocean: Numerical experiments using a wind-driven quasigeostrophic model. *J. Phys. Oceanogr.* **8**, 363–392.

Jacobsen, T. S. 1986. Water exchange through the Danish Straits. In: *Baltic Sea Environment Proc. no. 16*, 174 pp.

Kielmann, J. 1981. Grundlagen und Anwendung eines numerischen Modells der geschichteten Ostsee. *Ber. Inst. f. Meeresk.* (Kiel) (no. **87a/b**) 158/116pp.

Killworth, P., Stainforth, D., Webbs, D. J. and Paterson, S. M. 1989. *A free surface Bryan–Cox–Semtner model.* Inst. of Oceanogr. Sciences Deacon Laboratory Report, No. 270, 184 pp.

Killworth, P., Stainforth, D., Webbs, D. J. and Paterson, S. M. 1991. The development of a free-surface Bryan–Cox–Semtner ocean model. *J. Phys. Oceanogr.* **21**, 1333–1348.

Krauss, W. 1981. The erosion of the thermocline. *J. Phys. Oceanogr.* **11**, 415–433.

Krauss, W. and Brügge, B. 1991. Wind-produced water exchange between deep basins of the Baltic Sea. *J. Phys. Oceanogr.* **21** (no. 3), 373–384.

Large, W. and Pond, S. 1981. Open ocean momentum flux measurements in moderate to strong winds. *J. Phys. Oceanogr.* **11**, 324–336.

Lehmann, A. 1992. Ein dreidimensionales wirbelauflösendes Modell der Ostsee. *Ber. Inst. f. Meeresk.* (Kiel) (no. **231**), 104 pp.

Lenz, W. 1971. Monatskarten der Temperatur der Ostsee. *Ergänzungsheft zur Hydrographischen Zeitschrift*, Reihe ***B***, no. 11.

Magaard, L. and Rheinheimer, G. 1974. *Meereskunde der Ostsee*. Springer Verlag, Berlin, 269 pp.

Matthäus, W. 1977. Mittlere vertikale Wärmeaustauschkoeffizienten in der Ostsee. *Acta Hydrophysica* (Berlin) **XXII**, H.2, 73–92.

Matthäus, W. and Franck, 1992. Characteristics of major Baltic inflows – a statistical analysis. *Cont. Shelf Res.* **12**, 1375–1400.

Matthäus, W., Lass, H. U. and Tiesel, R. 1993. *The major Baltic inflow in January 1993.* ICES C.M. 1993/C:51.

Millero, F. J. and Kremling, K. 1976. The densities of Baltic Sea waters. *Deep Sea Res.* **23**, 1129–1138.

Millero, F. J., Gonzales, A. and Ward, G. K. 1976. The density of seawater solutions at one atmoshpere as a function of temperature and salinity. *Journal of Marine Res.* **34**, 61–93.

Munk, W. H. and Anderson, E. R. 1948. Notes on a theory of the thermocline. *J. Marine Res.* **VII**, 3., 276–295.

Omstedt, A. 1990. Modelling the Baltic Sea as thirteen sub-basins with vertical resolution. *Tellus* **42A**, 286–301.

Pacanowski, R. C. and Philander, S. G. 1981. Parameterization of vertical mixing in numerical models of tropical oceans. *J. Phys. Oceanogr.* **11**, 1443–1451.

Semtner, A. J. 1974. *A general circulation model for the World Ocean.* UCLA Dept. of Meteorology Tech. Rep. No. 8, 99pp.

Semtner, A. J. and Mintz, Y. H. 1977. Numerical simulation of the Gulf Stream and mid-ocean eddies. *J. Phys. Oceanogr.* **7**, 208–230.

Simons, T. J. 1978. Wind-driven circulations in the southwest Baltic. *Tellus* **30**, 272–283.

Stevens, D. P. 1991. The open boundary condition in the United Kingdom Fine-Resolution Antarctic Model. *J. Phys. Oceanogr.* **21**, 1494–1499.

Stigebrandt, A. 1993. A model for the exchange of water and salt between the Baltic and the Skagerrak. *J. Phys. Oceanogr.* **13**, 411–427.

Stigebrandt, A. 1987. A model of the vertical circulation of the Baltic deep water. *J. Phys. Oceanogr.* **17**, 1772–1785.

Wyrtki, K. 1953/1954. Die Dynamik der Wasserbewegungen im Fehmarnbelt I und II. *Kieler Meeresforsch.* **IX**, 155–170; **X**, 162–181.

Wyrtki, K. 1954. Der große Salzeinbruch in die Ostsee im November und Dezember 1951. *Kieler Meeresforsch.* **10**, 19–25.

Yin, F. L. and Fung, I. Y. 1991. Net diffusivity in ocean general circulation models with nonuniform grids. *J. Geophys. Res.* **96**, 10773–10776.